Published in final edited form as:
Biomaterials. 2008 February ; 29(4): 418–426.

A Microfabricated Scaffold for Retinal Progenitor Cell Grafting

William L. Neeley[1], **Stephen Redenti**[2], **Henry Klassen**[3], **Sarah Tao**[4], **Tejal Desai**[4], **Michael J. Young**[2], and **Robert Langer**[1,5,*]

1 *Department of Chemical Engineering, Massachusetts Institute of Technology, 77 Massachusetts Avenue, Cambridge, Massachusetts, U.S.A.*

2 *Schepens Eye Research Institute, Department of Ophthalmology, Harvard Medical School, 20 Staniford Street, Boston, Massachusetts, U.S.A.*

3 *Department of Ophthalmology, School of Medicine, University of California, Irvine, 101 The City Drive, Orange, California, U.S.A.*

4 *Department of Physiology, University of California, San Francisco, 1700 4th Street, San Francisco, California, U.S.A.*

5 *Harvard-MIT Division of Health Sciences and Technology, Massachusetts Institute of Technology, 77 Massachusetts Avenue, Cambridge, Massachusetts, U.S.A.*

Abstract

Diseases that cause photoreceptor cell degeneration afflict millions of people, yet no restorative treatment exists for these blinding disorders. Replacement of photoreceptors using retinal progenitor cells (RPCs) represents a promising therapy for the treatment of retinal degeneration. Previous studies have demonstrated the ability of polymer scaffolds to increase significantly both the survival and differentiation of RPCs. We report the microfabrication of a poly(glycerol-sebacate) scaffold with superior mechanical properties for the delivery of RPCs to the subretinal space. Using a replica molding technique, a porous poly(glycerol-sebacate) scaffold with a thickness of 45 μm was fabricated. Evaluation of the mechanical properties of this scaffold showed that the Young's modulus is about 5-fold lower and the maximum elongation at failure is about 10-fold higher than the previously reported RPC scaffolds. RPCs strongly adhered to the poly(glycerol-sebacate) scaffold, and endogenous fluorescence nearly doubled over a 2 day period before leveling off after 3 days. Immunohistochemistry revealed that cells grown on the scaffold for 7 days expressed a mixture of immature and mature markers, suggesting a tendency towards differentiation. We conclude that microfabricated poly(glycerol-sebacate) exhibits a number of novel properties for use as a scaffold for RPC delivery.

Keywords

progenitor cell; scaffold; retina; biocompatibility; elastomer

*To whom correspondence should be addressed: Telephone: 617-253-3107; Fax: 617-258-8827; E-mail: rlanger@mit.edu.

1. Introduction

Age-related macular degeneration (AMD) and retinitis pigmentosa (RP) are two major diseases of the retina that involve photoreceptor cell degeneration and frequently result in clinically apparent visual loss [1]. More than 1.75 million people in the United States have AMD, and this number is expected to grow to 2.95 million people by 2020 due to the aging population [2]. RP, an inherited disease, afflicts approximately 1 in 3700, or roughly 80,000 people in the United States [3]. Current treatments for wet AMD consist of laser photocoagulation, photodynamic therapy using the photosensitizing dye verteporfin (Visudyne®, Novartis), and anti-angiogenesis therapy using the oligonucleotide antagonist pegaptanib (Macugen®, Eyetech Pharmaceuticals and Pfizer) [4], the VEGF antibody fragment ranibizumab (Lucentis™, Genentech), and the VEGF antibody bevacizumab (Avastin™, Genentech). Preventative measures such as anti-oxidant supplements [5] and smoking cessation [6] also show some effectiveness. Only one therapy exists for RP, and it consists of taking vitamin A palmitate supplements (15000 IU per day) and maintaining a diet rich in omega-3 fatty acids while avoiding high doses of vitamin E (400 IU per day) as preventative measures [7,8]. At best, all of these therapies merely slow the progression of disease and, although Lucentis™ has been shown to restore some vision in 40% of patients with wet AMD, this outcome may result from temporarily rescuing dying photoreceptors [9]. Regardless, an approach is needed that can restore lost vision through replacement of photoreceptors that have been lost to the degenerative process.

One strategy to restore visual function in patients with retinal degeneration consists of replacing photoreceptor cells by grafting tissue to the retina. For this approach to succeed, the grafted cells must integrate into the host tissue. However, transplantation of differentiated neural tissue to the retina exhibits only limited evidence of integration [10]. Gage and coworkers demonstrated that central nervous system stem cells can overcome this problem and showed that adult rat hippocampus-derived neural progenitor cells integrate to a high degree in most layers of the retina when injected into the eyes of neonatal rats or mature rats with active retinal degeneration [11,12]. Although the hippocampus-derived neural progenitor cells differentiate to neurons with morphological similarities to the various retinal cells, including photoreceptors, complete differentiation does not occur. Consequently, Young and coworkers isolated retinal progenitor cells (RPCs) and showed that not only are they predisposed to differentiate into retinal neurons, but they also possess integrative abilities like those of brain-derived stem cells [13]. Transplantation of RPCs therefore represents a promising approach for photoreceptor replacement.

Formidable challenges exist for successfully grafting RPCs to the retina, including delivery, survival, and differentiation of the cells [14]. Recent studies show that the seeding of RPCs onto polymer scaffolds can address all three of these problems [15–17]. Typically, delivery is achieved by injection of cell suspensions into the subretinal space or into the vitreous cavity [14]; however, this technique can result in disorganized or incorrectly localized grafts and also contributes to poor cell survival due to shearing forces during injection and reflux of cells from the injection site. By contrast, delivering cells to the retina in the form of a degradable poly (lactic acid)/poly(lactic-*co*-glycolic acid) (PLA/PLGA) composite graft decreases the number of cells lost to reflux and/or shearing forces by nearly 50% and improves overall survival after 4 weeks by 10-fold over cell suspension grafts, corresponding to a survival rate of 78% [16]. The use of PLA/PLGA composite grafts also promotes differentiation of RPCs as evidenced by induction of morphological changes [15] and the expression of recoverin and rhodopsin (retina-specific membrane proteins) [16]. The encouraging results outlined above warrant further development of this technology. At present, significant improvements to the mechanical properties of the scaffold, the inflammatory response induced by the scaffold, and the ability

of the scaffold to differentiate the RPCs to functional photoreceptors are needed for this strategy to find use in the clinic.

We recently introduced poly(glycerol-sebacate) (PGS) as a biodegradable and elastomeric polymer for potential use in tissue engineering [18]. PGS possesses a number of properties that in principle make it well-suited for RPC delivery. A comparative study of PGS and PLGA demonstrated the superiority of PGS degradation and showed that PGS degrades by surface erosion, which results in preservation of geometry, no detectable swelling, and slow loss of mechanical strength relative to mass, whereas PLGA undergoes bulk degradation accompanied by extensive deformation, swelling, and faster loss of mechanical strength than mass [19]. Studies in vitro and in vivo demonstrate the improved biocompatibility of PGS relative to PLGA. Growth in culture of 3T3 human fibroblasts or rat Schwann cells, which are more sensitive than fibroblasts, proceeds as well or better on PGS than it does on PLGA [18,20]. In vivo, PGS induces less inflammation and fibrosis than PLGA and does not induce the foreign body giant cell response characteristic of PLGA [20]. Finally, the structure of PLGA allows for only facile modification on the ends of the polymer, whereas the plethora of carboxyl and hydroxyl groups within PGS chains (Figure 1) allows for decoration of the polymer with bioactive moieties through linkages such as ester, amide, ether, or acetal bonds. Together, these observations suggested that the performance and versatility of PGS would far surpass that of the previously used PLA/PGLA blend for RPC delivery. We report here the microfabrication of a porous PGS membrane for RPC delivery and the in vitro evaluation of PGS interaction with mouse RPCs (mRPCs).

2. Materials and Methods

2.1. Materials

Unless otherwise noted, all reagents were purchased from Sigma-Aldrich (St. Louis, MO) and used without further purification. PDMS (Sylgard 184) was from Dow Corning (Midland, MI). SU8-2050 was obtained from Microchem (Newton, MA). Silicon wafers were purchased from WaferNet (San Jose, CA).

2.2. Methods

2.2.1. Synthesis of PGS prepolymer—PGS was prepared as previously described [18]. Briefly, 200 g (0.989 moles) of sebacic acid and 91.1 g (0.989 moles) of anhydrous glycerol were charged to a flask and reacted at 120 °C under a stream of N_2. After 21 h, vacuum was applied and the mixture reacted for another 64 h. The extent of polymerization was determined by measuring the intrinsic viscosity of the product in acetone using an Ubbelohde viscometer (model 0C, constant 0.00298) (VWR, West Chester, PA). The intrinsic viscosity of PGS produced under the conditions described above was 0.095 ± 0.002 dL/g at 30 °C.

2.2.2. Microfabrication of PDMS—All fabrication procedures were carried out in a class 10000 clean room. An 80 μm thick layer of SU8-2050 was spin-coated on a silicon wafer (4 inch diameter) following the manufacturer's instructions. The photoresist was patterned using a transparency mask (PageWorks, Cambridge, MA) with the ink-side down and developed using washes of propylene glycol monomethyl ether acetate and isopropanol. The patterned silicon wafer was prepped for PDMS replica molding by treating with a low surface energy release agent (tridecafluoro-1,1,2,2-tetrahydrooctyl)trichlorosilane. Briefly, 2 drops of (tridecafluoro-1,1,2,2-tetrahydrooctyl)trichlorosilane were applied to a glass slide, which was placed on the floor of a vacuum chamber containing the patterned silicon wafer. A vacuum was applied and the (tridecafluoro-1,1,2,2-tetrahydrooctyl)trichlorosilane vapor allowed to react with the wafer for at least 20 minutes. The PDMS negative mold was prepared from the patterned silicon wafer as described [21].

2.2.3. Fabrication of PGS scaffolds—Fabrication of the PGS scaffolds was carried out in a class 10000 clean room. The PDMS negative mold was oxidized by plasma treatment for 1 min to create a hydrophilic surface [22–24]. A 61.5% aqueous sucrose solution (0.2 μm filtered) was spin coated at 3000 RPM for 30 sec on the oxidized PDMS mold within 5 minutes of plasma treatment. The sucrose-coated PDMS was immediately baked at 135 °C in an oven for 10 min and then transferred to a 120 °C hotplate. Approximately 6.5 g of molten PGS (150 °C) were spin coated at 3000 RPM for 30 sec on the sucrose-coated PDMS molds. The PGS on the PDMS mold was cured at 120 °C under a vacuum of 15 mTorr for 48 hr. Subsequently, the mold was submerged in ddH_2O for 16 days to loosen the PGS from the PDMS mold. The PGS was precut into pieces using a razorblade, and the pieces were gently peeled off the PDMS mold using forceps. To examine the PGS scaffold by SEM, the scaffold was coated with Au/Pd using an evaporator.

2.2.4. Mechanical testing—The mechanical properties of the PGS scaffolds were determined using an Instron 5542 testing system. Strips of PGS scaffold measuring approximately 12 mm × 6 mm × 45 μm were prepared using a razorblade. Because of the small dimensions of the test strips, grip failures during testing could be problematic. Consequently, the test strips were attached to glass slides, which served as the attachment points for the instrument grips. The testing apparatus was prepared as follows. Two glass microscope slides were held together end-to-end by clips, and the ends were separated such that an approximately 7 mm gap was formed between the two slides. The PGS scaffold test strip was suspended between the two slides, and the ends of the PGS scaffold strip were attached to the glass using cyanoacrylate glue. The clips were removed from the glass slides after securing the glass slides in the instrument grips. Prior to testing, the exact length and width of the test strips were measured using a digital caliper. The scaffolds were tested at a constant strain rate of 2 mm/min until failure. The results are reported as the average of four successful tests.

2.2.5. Progenitor cell isolation and culture—All experiments were performed according to the guidelines of the Schepens Eye Research Institute and Massachusetts Institute of Technology Animal Care and Use Committees and the ARVO Statement for the Use of Animals in Ophthalmic and Vision Research. Green fluorescent protein positive (GFP+) mouse retinal progenitor cells (mRPCs) were isolated from day P0 retinas as previously described [13]. Briefly, isolated RPCs were cultured at 37 °C in NB complete medium, which contained 2% (v/v) B27 neural supplement (Invitrogen-Gibco, Rockville, MD), 1% (v/v) N2 supplement (Invitrogen-Gibco), 100 μg/mL Pen/Strep (Sigma-Aldrich), 2 mM L-glutamine (Sigma-Aldrich), 20 units/mL Nystatin (Sigma-Aldrich), and 20 ng/mL recombinant human epidermal growth factor (rhEGF) (Promega, Madison, WI) in NeuroBasal medium (Invitrogen-Gibco). Cells were allowed to proliferate for six weeks and then passaged 1:3 every two weeks.

2.2.6. PGS culture preparation—PGS scaffold sections (5 × 5 mm) were sterilized by submersion in 70% ethanol for 2-4 hours and then rinsed 4 × 15 min in PBS under sterile conditions. PGS scaffolds were then transferred to a sterile 12-well plate (Multiwell, Becton Dickinson Labware, Franklin Lakes, NJ) and incubated in 0.1 mg/mL laminin in PBS for 2 h and then rinsed 3 times in sterile PBS. The scaffolds were subsequently transferred to a 0.4 μm pore culture well insert (BD Biosciences, San Jose, CA) and submerged in 1 mL of fresh NB complete medium for 1 h at 37 °C, prior to seeding.

2.2.7. Seeding and attachment of mRPCs to PGS—GFP+ mRPCs cultured in a T-75 flask containing 10 mL of NB complete medium were transferred to a 15 mL Falcon tube and centrifuged at 850 × g for 3 min. The supernatant was removed and the remaining mRPC pellet resuspended in 4 mL of NB complete medium warmed to 37 °C. One mL of mRPC supernatant at a concentration of approximately 5×10^5 cells/mL was added to the PGS scaffold in the

culture insert and incubated at 37 °C for 24 h. The PGS/mRPC composites were transferred to new 12-well plates containing 2 mL of NB complete medium every 24 h until a total of 4 days had passed since the initial seeding. This procedure was done to evaluate the degree to which mRPCs adhered to, or were retained within the pores of, the scaffolds. After this time, the composites were no longer transferred and were cultured in the final well until 7 days had passed since the initial seeding. This approach allowed for assessment of the growth potential of GFP+ mRPCs on the scaffold surface.

2.2.8. Analysis of GFP+ mRPC proliferation on PGS—The composites were imaged at 10X magnification every 24 h from 48 to 168 h after the initial seeding of cells using a Spot ISA-CE camera (Diagnostic Instruments, Sterling Heights, CA) attached to a Nikon Eclipse TE800 microscope. Images were then analyzed for changes in fluorescence intensity using Image J software (National Institutes of Health). Changes in mRPC-associated GFP fluorescence were measured as an indicator of cell survival and proliferation.

2.2.9. Immunohistochemistry—After culturing for 7 days, composites and single cells adherent to laminin-coated slides were rinsed 3 times with PBS (warmed to 37 °C) and fixed in 4% paraformaldehyde for 1 h. A second set of composites was fixed in 4% paraformaldehyde, cryoprotected first in 10% sucrose for 12 h and then in 30% sucrose for 12 h. Cryoprotected composites were frozen in Optimal Cutting Temperature Compound (Sakura Finetek, Torrence, CA) at −20°C and sectioned at 20 μm using a Minotome Plus (Triangle Biomedical Sciences, Durham, NC). All samples were rinsed 3 × 10 min in PBS and then blocked and permeabilized in PBS containing 10% goat serum, 1% BSA, and 0.1% Triton-x for 2 h. Samples were incubated with primary antibodies using a dilution of 1:200 for MAP-2 (Sigma), 1:1000 for nf-200 (Sigma), 1:200 for GFAP (Zymed, San Francisco, CA), 1:1000 for recoverin (Chemicon, Temecula, CA), 1:500 for PKC (Santa Cruz Biotech, Santa Cruz, CA), 1:400 for nestin (BD Biosciences), 1:100 for Ki67 (Vector Laboratories, Burlingame, CA), and 1:200 for Rho-4D2 (a gift from Prof. Robert Molday, University of British Columbia, Canada) in blocking buffer for 12 h at 4 °C. Samples were then rinsed 3 × 10 min in PBS and incubated with a Cy3-labeled secondary antibody 1:800 (Zymed) for 2 h at room temperature. Finally, samples were rinsed 3 × 10 min in PBS and sealed in mounting medium (Vector Laboratories) for imaging using a Leica TCS SP2 confocal microscope.

3. Results

3.1. Scaffold fabrication and properties

In choosing the fabrication method, we sought a technique that would allow precise control over the size and pattern of pores to allow for future experimentation involving variation of these parameters in a predictable fashion. Thus, a replica molding technique was used to fabricate the porous PGS scaffold (Figure 2). Using this procedure, the scaffold pattern can be designed on a computer and then translated into a flexible PDMS negative mold using standard microfabrication technology. At this stage, two main problems inhibit the soft lithography of PGS on PDMS. Firstly, when cured on a substrate, PGS tends to adhere to the substrate material thereby preventing intact removal of the PGS from the substrate. Secondly, molten PGS does not spread evenly on a PDMS surface and instead repels from the surface, most likely due to interaction between the hydrophobic PDMS and the comparatively hydrophilic PGS. We reasoned that applying a sacrificial coating between the PDMS and PGS could solve both problems. Because PDMS swells upon exposure to organic solvents [25] and residual solvents in polymer scaffolds can be toxic to cells, the use of a water soluble release agent was desirable. Plasma oxidation of PDMS creates a hydrophilic surface [26] and we hypothesized that this property could be used to apply a layer of an aqueous solution to the surface of the PDMS. Indeed, spin-coating oxidized PDMS with an aqueous sucrose solution resulted in the

formation of a thin layer of sucrose. Molten PGS was then spin-coated on top of the dried sucrose layer forming a layer that remained spread on the surface. Upon curing of the PGS, no apparent change in the uniformity of the PGS layer occurred. Submersion of the coated PDMS mold in water dissolved the sucrose layer and allowed delamination of the cured PGS scaffold from the PDMS mold.

Previous studies with PLA/PLGA utilized solid-liquid phase separation to generate a highly porous structure with pore diameters of about 35–50 μm and a sheet thickness of minimum 150 μm [16]. The pore size of these scaffolds appears to work well in this example, thus we chose 50 μm pores as the starting point for fabricating PGS scaffolds. Typically, cells must be within 200 μm of a nutrient source, such as a capillary vessel [27]. Consequently, the scaffold pores were spaced so that every cell attached to the scaffold would be well within this distance from a pore opening. The anatomy of the retina also influenced the design of the scaffold. The human retina averages 360 μm thick [28], so we sought to produce a scaffold significantly thinner than the previously reported 150 μm scaffold to minimize perturbation of the retina. Additionally, retinal detachments can lead to permanent vision loss as a result of photoreceptor cell death [29,30]. This outcome occurs because photoreceptors receive their nutrient supply by diffusion from the choriocapillaris, and this supply is disrupted by the retinal detachment. By contrast, the inner layers of the retina are supplied by the retinal circulation, which is not affected by the detachment [31]. Thus, decreasing the thickness of the porous scaffold should reduce the risk of photoreceptor starvation. Using the method in Figure 2, we produced a scaffold with a thickness of approximately 45 μm containing 50 μm pores spaced 175 μm apart, center to center (Figure 3). Examination of the PGS scaffold by SEM indicated that the replica molding method imparted a raised region around the pore openings that we attribute to capillary action between the sucrose and PGS layers and the PDMS posts.

Testing of the scaffold mechanical properties indicated that the porous PGS scaffold was an elastic and soft material with a maximum strain at failure of 113 ± 22% and a Young's modulus of 1.66 ± 0.23 MPa. Figure 4 depicts a representative stress-strain curve for the PGS scaffold.

3.2. Seeding and adhesion of mRPCs on PGS

As described in Methods, scaffolds were incubated with 0.1% laminin prior to RPC seeding. To assess the ability of mRPCs to remain adherent to the scaffolds, cell-scaffold composites were successively transferred to new culture wells. These manipulations produced no significant difference in the relative fluorescence of the composite samples, which remained steady at the baseline levels seen in Figure 5 (relative fluorescence = 14 ± 2). These results can be attributed to the retention of GFP+ cells within the pores of the scaffold, together with loss of nascent cells during transfers due to shearing of cells from the scaffold surface [17]. The composites were subsequently left undisturbed in culture whereupon the amount of relative fluorescence nearly doubled over a 48 h period before leveling off over the final 24 h of culturing (Figure 5). Confocal microscopy performed after 7 days of culture revealed extensive infiltration of the scaffold pores by mRPCs (Figure 6). Cross-sectional views of the cell-scaffold composite (Figure 6, panels in) confirmed the presence of cells throughout the pores and also revealed substantial adhesion of cells to the external surfaces of the scaffolds (Figure 6, panels ah, m, n).

3.3. Expression of phenotypic markers

The protein expression patterns of mRPCs grown for 7 days on a PGS scaffold were analyzed by immunohistochemistry (Figure 6). This work revealed expression of the primitive neuroepithelial marker nestin (c), the astroglial marker GFAP (f), and the neuronal marker neurofilament-200 (h). No expression of MAP-2 (a), the proliferation marker Ki67 (d), or the

retinal cell-specific markers protein kinase C-α (b), rhodopsin (e), or recoverin (g) was detected.

4. Discussion

Several studies have demonstrated the potential of using a polymer scaffold to deliver RPCs to the mammalian retina [15,16,32,33]. One of these studies examined the use of a non-degradable poly(methyl methacrylate) (PMMA) scaffold [17], whereas the other three focused on a degradable PLA/PLGA scaffold [15,16,33]. Two specific limitations of the previously reported degradable scaffolds, the mechanical properties and thickness of the scaffold, are addressed in the present work with the goal of further developing this technology in anticipation of clinical use. The use of a degradable scaffold is advantageous to the extent that bioabsorption of the foreign material allows the local microenvironment to return to a homeostatic state. PGS has potential in the setting of structured cell delivery due to its inherent toughness and flexibility [18]. In assessing the utility of PGS as a material for the construction of RPC-containing scaffolds, it was determined that a method was needed for the fabrication of thin and porous PGS membranes. Given that the use of PGS as a polymer in tissue engineering was proposed only recently [18], there are a limited number of studies reporting the fabrication of porous scaffolds using this polymer [34–37]. The fabrication methods used in those reports utilized a classical salt-leaching approach for the creation of scaffolds with high porosity, yet irregular pore structure. Recent work suggests that the fabrication of scaffolds with precise control of pore structure and porosity results in improved mechanical properties and increased reproducibility [38]. For the present work a fabrication strategy was therefore developed utilizing micropatterned PDMS that allowed the creation of a thin PGS scaffold with precisely defined pores. Importantly, scaffolds of varying porosity and pore structure can be quickly and easily produced using this platform method, which will enable future systematic examinations of the relation between scaffold design, RPC growth, and grafting to the eye.

The mechanical properties of a scaffold are critical for successful surgical implantation. The PLA/PLGA blend used in previous studies has an elastic modulus of 9.0 ± 1.7 MPa and a maximum strain at failure of only about 9% [15], whereas retinal tissue has an elastic modulus of 0.1 MPa and a maximum strain at failure of about 83% [39]. These data indicate that the PLA/PLGA blend is a hard and brittle material in comparison to retinal tissue, which limits the degree of manipulation the scaffolds may experience during implantation and increases the likelihood of tissue injury due to noncompliance. Alternatively, the PGS scaffold reported in this work possesses significantly improved mechanical properties that are more similar to those of retinal tissue. The loss of mechanical strength relative to mass is an especially important parameter for selection of a biodegradable polymeric scaffold since seeding of the polymer with cells requires immersion of the polymer in media for approximately one week prior to implantation. A recent study showed that PLGA loses >98% of its mechanical strength after 7 days in vivo, which is typical for bulk degrading polymers, whereas PGS loses only about 8% over the same time period despite a greater loss in mass [19]. Significant loss of mechanical strength during cell seeding impedes polymer implantation because of the increased fragility of the scaffold. Tomita et al. proposed a minimally invasive method for cell-scaffold composite delivery that would involve rolling the composite into a scroll-like structure that is injected into the subretinal space where it would then unfold. For scaffolds of equivalent length and width, the invasiveness of this technique is proportional to the thickness of the composite. By employing spin-coating in the PGS scaffold fabrication procedure, we were able to reduce the thickness of the RPC scaffold from 150 μm in the case of the PLA/PLGA scaffold [16] to approximately 45 μm for the PGS scaffold. Initial studies with the PGS scaffold reported here indicate that it can easily accommodate the manipulations required for the minimally invasive implantation procedure described above.

The subretinal space represents an immune privileged site [40], and this characteristic provides a conducive environment for delivery of mRPCs on a scrollable PGS scaffold. In addition, mRPCs do not express MHC class I or II antigens and can be classified as an immunoprivileged cell type [10]. Consequently, mRPCs injected into the subretinal space of allogeneic recipients survive and integrate without eliciting an immunogenic response. An increasing number of biodegradable polymers including PLGA, poly(glycolic acid), poly(lactic acid), and polycaprolactone have demonstrated biocompatibility with the retinal environment [14]. Studies using the polymers PLA/PLGA and PMMA as vehicles for subretinal mRPC delivery report enhanced cell delivery and survival, along with biocompatibility in the retina and posterior eye of rodents [16,17]. Exploration of the biocompatibility of transplanted retinal progenitors within the host retina has recently been advanced to a porcine model that more closely resembles human biology and surgical anatomy [41]. Porcine retinal progenitor cells (pRPCs) are also more genetically homologous to human RPCs than murine RPCs. The survival of transplanted pRPCs is substantial at two weeks and variable at five weeks in the absence of an observable immune response [41]. Both porcine and mouse RPCs transplanted to the allogeneic retina expressed markers for mature retinal cell types within weeks [16,41, 42]. PLA/PLGA scaffolds resulted in an increased organization of xenografted mRPCs beneath the pig retina, although this was associated with a local foreign body response [29].

It is common for cultured populations of multipotent RPCs to express simultaneously both immature and mature markers, with individual cells changing expression toward a specific cell fate after exit from the cell cycle [16,43]. Previous studies show that both seeding of progenitor cells onto polymer scaffolds and transplantation to the retina result in changes in gene expression [15,16]. In this study, the markers nestin, neurofilament-200 (nf-200), and GFAP were expressed by mRPCs grown on PGS scaffolds. These markers suggest the presence of a heterogeneous population of cell types at the 7 day time point. The neuroectodermal marker nestin is indicative of a subpopulation of relatively undifferentiated progenitors [43], whereas expression of nf-200 suggests the presence of more mature cells of neuronal lineage. GFAP expression is less specific in the present context but is generally consistent with cells of glial lineage, either radial glial, astrocytes, or activated Müller cells. The lack of Ki67 expression suggests an absence of actively proliferating cells, while the absence of the mature neuronal and retinal markers MAP-2, recoverin, and rhodopsin suggests an absence of mature retinal cell types. Taken together, the data can be interpreted as showing partial differentiation in which 7 days in culture on PGS has resulted in widespread exit from the cell cycle but is as yet insufficient to result in terminal differentiation. The extent to which this interpretation is correct remains to be fully evaluated. Interestingly, growth of mRPCs on the PGS scaffold appeared to level off prior to the 7 day time point (Figure 5), consistent with the notion that cellular proliferation had slowed considerably at this time.

One aspect of an RPC-based therapy that will need to be addressed in vivo is synaptogenesis. Previous work with PLA/PLGA scaffolds did not assay for the formation of functional synapses after differentiation of the grafted RPCs [16]. However, another study by Young and coworkers using the same cells (cultured postnatal day 1 RPCs) delivered by bolus injection noted differentiation of the cells into presumptive photoreceptor cells and observed improvement in light-mediated behavior [13], thereby raising the possibility that the cells may be able to form functional synaptic connections when placed in the proper environment. A recent study by MacLaren et al. used a similar approach and reported the formation of synaptic connections accompanied by improved visual function [44]. The authors found that the cells responsible for these results were not proliferating progenitor cells but rather post-mitotic rod precursor cells expressing the rod-specific transcription factor Nrl [45,46]. Only about 0.1% of the injected cells integrated into the host retina and differentiated into photoreceptor cells, which underscores the need to improve the efficiency of this strategy. The use of nonproliferating cells for a clinical therapy is both desirable, since it enhances safety, and problematic, since it

requires a constant resupply of suitable donor tissue. Ex vivo expansion of proliferating donor cells overcomes the problem of tissue supply, and the apparent capacity of polymer scaffolds to induce changes in co-cultured progenitor cells toward a more differentiated phenotype could therefore represent an important advantage of using polymer scaffolds, particularly in the context of clinical transplantation.

5. Conclusions

A platform for the microfabrication of a thin, porous PGS scaffold was developed for RPC grafting. The mechanical properties of the PGS scaffold reported here resemble those of retinal tissue and represent a significant improvement over the mechanical properties of previously reported scaffolds for this application. Additionally, the thickness of the scaffold was greatly reduced over previous examples, which is essential for the clinical utility in this setting. In vitro studies indicated that RPCs adhere to and proliferate on PGS. The expression of nestin and nf-200 indicate the potential for cell expansion while the expression of GFAP may indicate a trend toward differentiation. Future work will focus on evaluating the performance of RPC-PGS composites in vivo.

Acknowledgements

We thank Kurt Broderick for assistance with photolithography, Dr. Anthony Garratt-Reed for assistance with SEM, and Lenny Li for assistance with immunohistochemistry and proliferation analysis. Financial support was provided by NIH grants DE013023 and HL060435, the Richard and Gail Siegal Gift Fund, the Foundation Fighting Blindness, the Department of Defense, and a grant from the Lincy Foundation (H.K., M.J.Y.). W.L.N. was supported by the NIH under Ruth L. Kirschstein National Research Service Award 1 F32 EY018285-01 from the National Eye Institute. S.R. was supported in part through Harvard Medical School, Molecular Basis of Eye Diseases, National Eye Institute Award T32 EY07145-06.

References

1. Margalit E, Sadda SR. Retinal and optic nerve diseases. Artif Organs 2003;27(11):963–74. [PubMed: 14616515]
2. Friedman DS, O'Colmain BJ, Munoz B, Tomany SC, McCarty C, de Jong PT, et al. Prevalence of age-related macular degeneration in the United States. Arch Ophthalmol 2004;122(4):564–72. [PubMed: 15078675]
3. Boughman JA, Conneally PM, Nance WE. Population genetic studies of retinitis pigmentosa. Am J Hum Genet 1980;32(2):223–35. [PubMed: 7386458]
4. Bylsma GW, Guymer RH. Treatment of age-related macular degeneration. Clin Exp Optom 2005;88 (5):322–34. [PubMed: 16255691]
5. Group A-REDSR. A randomized, placebo-controlled, clinical trial of high-dose supplementation with vitamins C and E, beta carotene, and zinc for age-related macular degeneration and vision loss: AREDS report no. 8. Arch Ophthalmol 2001;119(10):1417–36. [PubMed: 11594942]
6. The Eye Disease Case-Control Study Group. Risk factors for neovascular age-related macular degeneration. Arch Ophthalmol 1992;110(12):1701–8. [PubMed: 1281403]
7. Berson EL, Rosner B, Sandberg MA, Hayes KC, Nicholson BW, Weigel-DiFranco C, et al. A randomized trial of vitamin A and vitamin E supplementation for retinitis pigmentosa. Arch Ophthalmol 1993;111(6):761–72. [PubMed: 8512476]
8. Berson EL, Rosner B, Sandberg MA, Weigel-DiFranco C, Moser A, Brockhurst RJ, et al. Further evaluation of docosahexaenoic acid in patients with retinitis pigmentosa receiving vitamin A treatment: subgroup analyses. Arch Ophthalmol 2004;122(9):1306–14. [PubMed: 15364709]
9. Heier JS, Antoszyk AN, Pavan PR, Leff SR, Rosenfeld PJ, Ciulla TA, et al. Ranibizumab for treatment of neovascular age-related macular degeneration: a phase I/II multicenter, controlled, multidose study. Ophthalmology 2006;113(4):642–4. [PubMed: 16483659]
10. Klassen H, Sakaguchi DS, Young MJ. Stem cells and retinal repair. Prog Retin Eye Res 2004;23(2): 149–81. [PubMed: 15094129]

11. Takahashi M, Palmer TD, Takahashi J, Gage FH. Widespread integration and survival of adult-derived neural progenitor cells in the developing optic retina. Mol Cell Neurosci 1998;12(6):340–8. [PubMed: 9888988]
12. Young MJ, Ray J, Whiteley SJ, Klassen H, Gage FH. Neuronal differentiation and morphological integration of hippocampal progenitor cells transplanted to the retina of immature and mature dystrophic rats. Mol Cell Neurosci 2000;16(3):197–205. [PubMed: 10995547]
13. Klassen HJ, Ng TF, Kurimoto Y, Kirov I, Shatos M, Coffey P, et al. Multipotent retinal progenitors express developmental markers, differentiate into retinal neurons, and preserve light-mediated behavior. Invest Ophthalmol Vis Sci 2004;45(11):4167–73. [PubMed: 15505071]
14. Young MJ. Stem cells in the mammalian eye: a tool for retinal repair. APMIS 2005;113(11–12):845–57. [PubMed: 16480454]
15. Lavik EB, Klassen H, Warfvinge K, Langer R, Young MJ. Fabrication of degradable polymer scaffolds to direct the integration and differentiation of retinal progenitors. Biomaterials 2005;26 (16):3187–96. [PubMed: 15603813]
16. Tomita M, Lavik E, Klassen H, Zahir T, Langer R, Young MJ. Biodegradable polymer composite grafts promote the survival and differentiation of retinal progenitor cells. Stem Cells 2005;23(10): 1579–88. [PubMed: 16293582]
17. Tao S, Young C, Redenti S, Zhang Y, Klassen H, Desai T, et al. Survival, migration and differentiation of retinal progenitor cells transplanted on micro-machined poly(methyl methacrylate) scaffolds to the subretinal space. Lab Chip 2007;7(6):695–701. [PubMed: 17538710]
18. Wang Y, Ameer GA, Sheppard BJ, Langer R. A tough biodegradable elastomer. Nat Biotechnol 2002;20(6):602–6. [PubMed: 12042865]
19. Wang Y, Kim YM, Langer R. In vivo degradation characteristics of poly(glycerol sebacate). J Biomed Mater Res A 2003;66(1):192–7. [PubMed: 12833446]
20. Sundback CA, Shyu JY, Wang Y, Faquin WC, Langer RS, Vacanti JP, et al. Biocompatibility analysis of poly(glycerol sebacate) as a nerve guide material. Biomaterials 2005;26(27):5454–64. [PubMed: 15860202]
21. Duffy DC, McDonald JC, Schueller OJA, Whitesides GM. Rapid prototyping of microfluidic systems in poly(dimethylsiloxane). Anal Chem 1998;70(23):4974–84.
22. Morra M, Occhiello E, Marola R, Garbassi F, Humphrey P, Johnson D. On the aging of oxygen plasma-treated polydimethylsiloxane surfaces. J Colloid Interface Sci 1990;137(1):11–24.
23. Chaudhury MK, Whitesides GM. Correlation between surface free energy and surface constitution. Science 1992;255(5049):1230–2. [PubMed: 17816829]
24. Chaudhury MK, Whitesides GM. Direct measurement of interfacial interactions between semispherical lenses and flat sheets of poly(dimethylsiloxane) and their chemical derivatives. Langmuir 1991;7(5):1013–25.
25. Lee Jessamine N, Park C, Whitesides George M. Solvent compatibility of poly(dimethylsiloxane)-based microfluidic devices. Anal Chem 2003;75(23):6544–54. [PubMed: 14640726]
26. Hollahan JR, Carlson GL. Hydroxylation of poly(methylsiloxane) surfaces by oxidizing plasmas. J Appl Polym Sci 1970;14(10):2499–508.
27. Colton CK. Implantable biohybrid artificial organs. Cell Transplant 1995;4(4):415–36. [PubMed: 7582573]
28. Shahidi M, Zeimer RC, Mori M. Topography of the retinal thickness in normal subjects. Ophthalmology 1990;97(9):1120–4. [PubMed: 2104523]
29. Arroyo JG, Yang L, Bula D, Chen DF. Photoreceptor apoptosis in human retinal detachment. Am J Ophthalmol 2005;139(4):605–10. [PubMed: 15808154]
30. Cook B, Lewis GP, Fisher SK, Adler R. Apoptotic photoreceptor degeneration in experimental retinal detachment. Invest Ophthalmol Vis Sci 1995;36(6):990–6. [PubMed: 7730033]
31. Mervin K, Valter K, Maslim J, Lewis G, Fisher S, Stone J. Limiting photoreceptor death and deconstruction during experimental retinal detachment: the value of oxygen supplementation. Am J Ophthalmol 1999;128(2):155–64. [PubMed: 10458170]
32. Tang H, Wang CC, Blankschtein D, Langer R. An investigation of the role of cavitation in low-frequency ultrasound-mediated transdermal drug transport. Pharm Res 2002;19(8):1160–9. [PubMed: 12240942]

33. Warfvinge K, Kiilgaard JF, Lavik EB, Scherfig E, Langer R, Klassen HJ, et al. Retinal progenitor cell xenografts to the pig retina: morphologic integration and cytochemical differentiation. Arch Ophthalmol 2005;123(10):1385–93. [PubMed: 16219730]
34. Radisic M, Park H, Chen F, Salazar-Lazzaro JE, Wang Y, Dennis R, et al. Biomimetic approach to cardiac tissue engineering: Oxygen carriers and channeled scaffolds. Tissue Eng 2006;12(8):2077–91. [PubMed: 16968150]
35. Gao J, Crapo Peter M, Wang Y. Macroporous elastomeric scaffolds with extensive micropores for soft tissue engineering. Tissue Eng 2006;12(4):917–25. [PubMed: 16674303]
36. Fidkowski C, Kaazempur-Mofrad MR, Borenstein J, Vacanti JP, Langer R, Wang Y. Endothelialized microvasculature based on a biodegradable elastomer. Tissue Eng 2005;11(1–2):302–9. [PubMed: 15738683]
37. Motlagh D, Yang J, Lui KY, Webb AR, Ameer GA. Hemocompatibility evaluation of poly(glycerol-sebacate) in vitro for vascular tissue engineering. Biomaterials 2006;27(24):4315–24. [PubMed: 16675010]
38. Hollister SJ. Porous scaffold design for tissue engineering. Nat Mater 2005;4(7):518–24. [PubMed: 16003400]
39. Wollensak G, Spoerl E. Biomechanical characteristics of retina. Retina 2004;24(6):967–70. [PubMed: 15579999]
40. Streilein JW. Ocular immune privilege and the Faustian dilemma. The Proctor lecture. Invest Ophthalmol Vis Sci 1996;37(10):1940–50. [PubMed: 8814133]
41. Klassen H, Kiilgaard JF, Zahir T, Ziaeian B, Kirov I, Scherfig E, et al. Progenitor cells from the porcine neural retina express photoreceptor markers after transplantation to the subretinal space of allorecipients. Stem Cells 2007;25(5):1222–30. [PubMed: 17218397]
42. Reh TA. Neurobiology: right timing for retina repair. Nature 2006;444(7116):156–7. [PubMed: 17093406]
43. Livesey FJ, Young TL, Cepko CL. An analysis of the gene expression program of mammalian neural progenitor cells. Proc Natl Acad Sci U S A 2004;101(5):1374–9. [PubMed: 14734810]
44. MacLaren RE, Pearson RA, MacNeil A, Douglas RH, Salt TE, Akimoto M, et al. Retinal repair by transplantation of photoreceptor precursors. Nature 2006;444(7116):203–7. [PubMed: 17093405]
45. Mears AJ, Kondo M, Swain PK, Takada Y, Bush RA, Saunders TL, et al. Nrl is required for rod photoreceptor development. Nat Genet 2001;29(4):447–52. [PubMed: 11694879]
46. Swain PK, Hicks D, Mears AJ, Apel IJ, Smith JE, John SK, et al. Multiple phosphorylated isoforms of NRL are expressed in rod photoreceptors. J Biol Chem 2001;276(39):36824–30. [PubMed: 11477108]

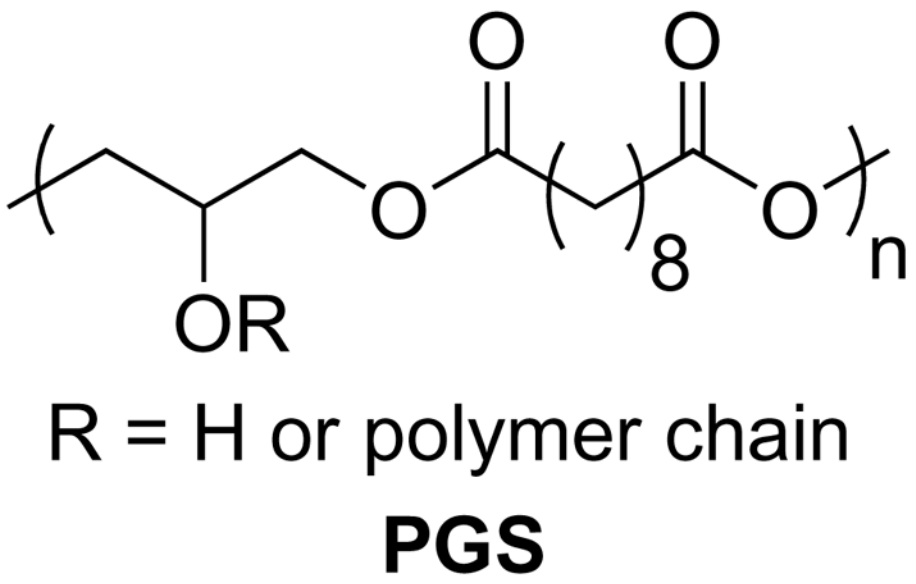

Figure 1.
Structure of poly(glycerol-sebacate).

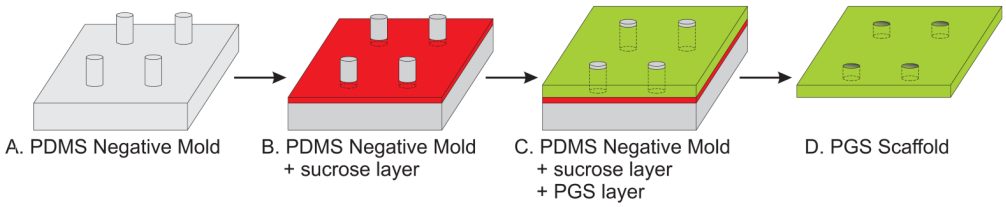

Figure 2.

Replica molding procedure for fabricating PGS scaffolds. (A) PDMS negative molds with 50 μm diameter × 80 μm tall pillars were created from a photopatterned silicon master. (B) Following plasma oxidation, the PDMS mold was spin-coated with an aqueous sucrose layer. (C) Molten PGS was spin-coated onto the sucrose-coated mold and cured in a vacuum oven. (D) The PGS layer was removed from the mold after incubation of the mold in water. The resultant scaffold contained 50 μm pores spaced 175 μm apart (center-to-center).

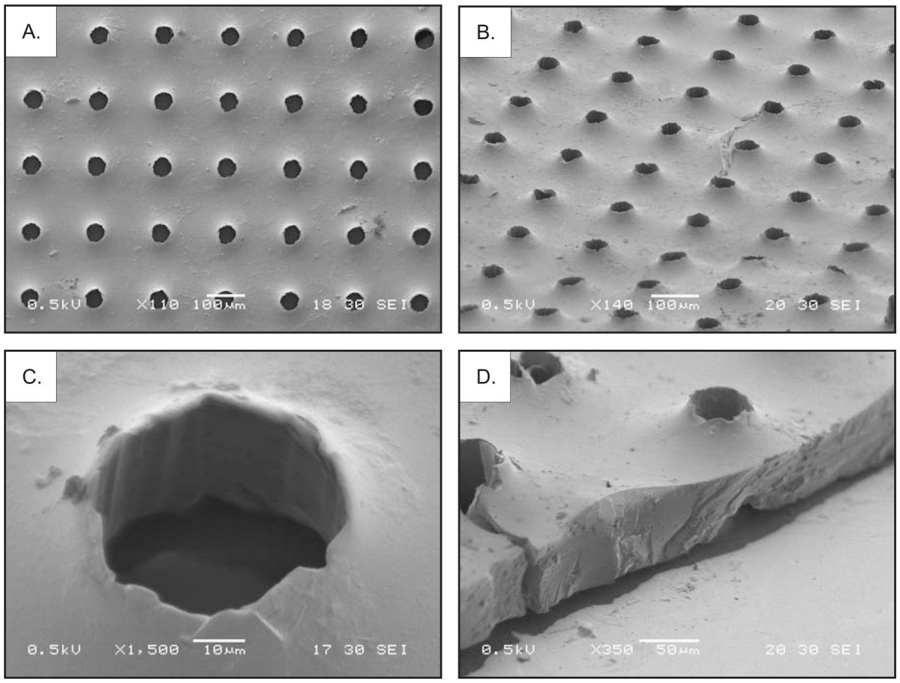

Figure 3.
Scanning electron microscope images of the PGS scaffold. (A) Top view of the scaffold. (B) View of the scaffold at a 60° angle. (C) Magnified view of a pore at a 30° angle. (D) Edge view of the scaffold at a 60° angle.

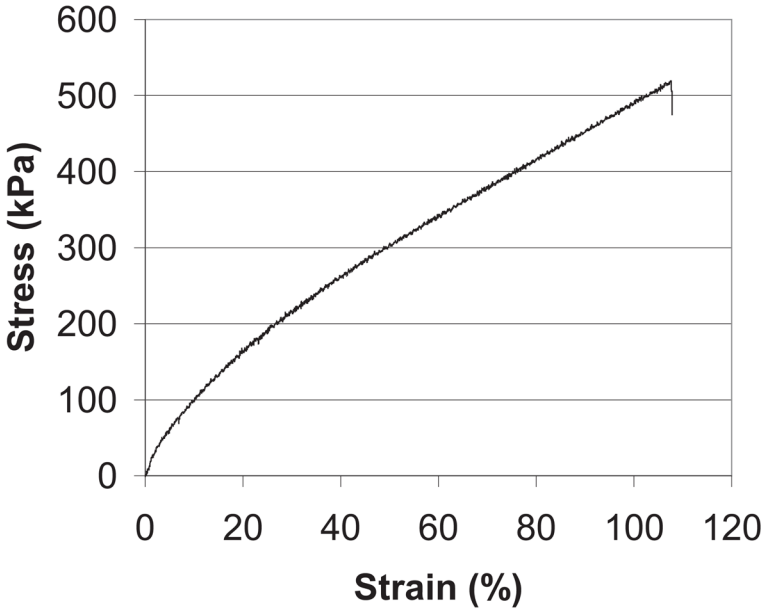

Figure 4.
Representative stress-strain curve for the PGS scaffold.

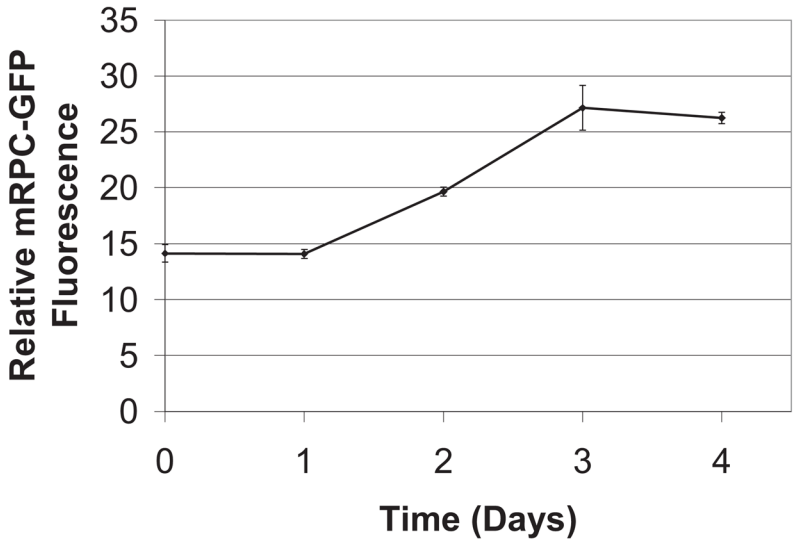

Figure 5.
Growth of GFP+ mouse retinal progenitor cells (mRPCs) on porous poly(glycerol-sebacate) (PGS). Relative GFP fluorescence was assessed over a 5 day period. PGS scaffolds pre-coated with mRPCs exhibited a nearly two-fold increase in GFP fluorescence above the initial baseline by day 3 of the observation period.

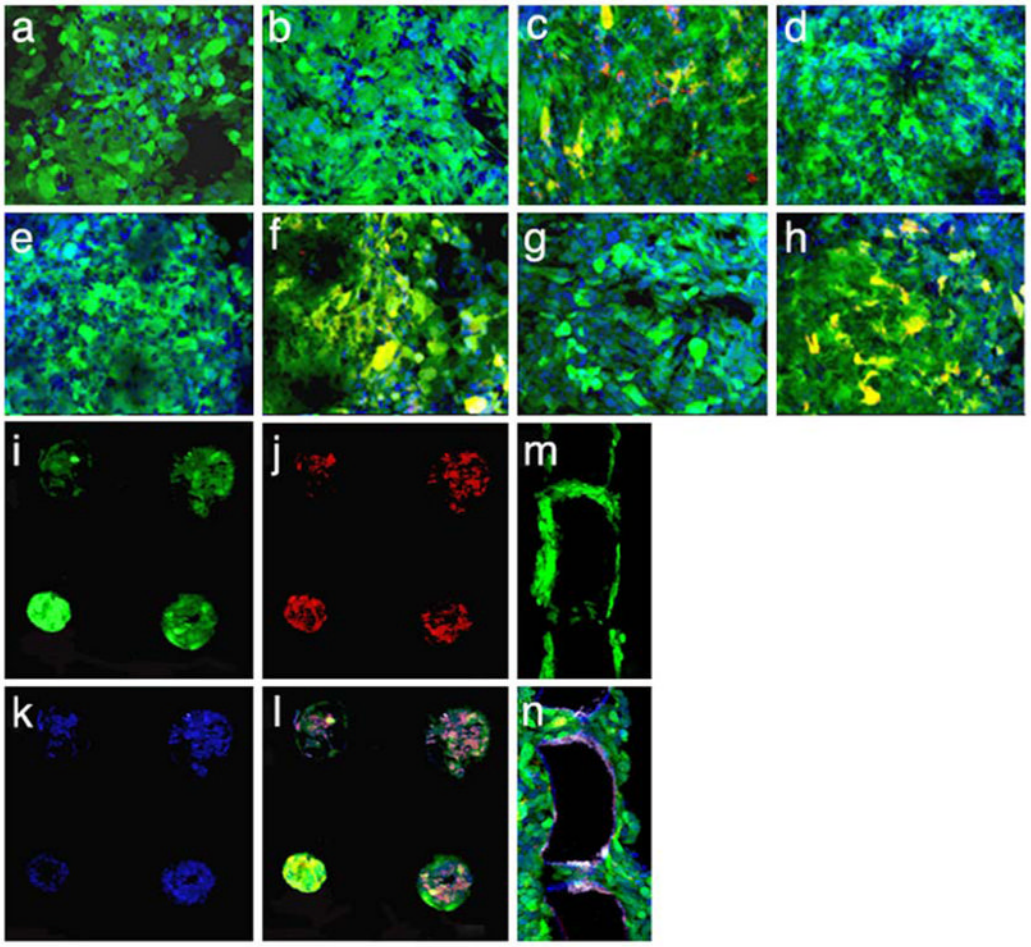

Figure 6.

Immunohistochemical characterization of GFP+ mouse retinal progenitor cells (mRPCs) cultured on porous poly(glycerol-sebacate) (PGS) substrates for one week using antibodies directed against: (a) the neuronal marker microtubule associated protein 2 (MAP-2), (b) the retinal bipolar cell marker protein kinase C (PKC), (c) the neurodevelopmental marker nestin, (d) the cell cycle-related marker Ki67, (e) the rod photoreceptor marker rhodopsin (Rho 4D2), (f) the astroglial and developmental marker glial fibrillary acidic protein (GFAP), (g) the retinal marker recoverin, and (h) the neuronal marker neurofilament-200 (nf-200). Of the above markers, nestin, GFAP, and nf-200 were positive for mRPCs grown on PGS. Each image is overlayed green = endogenous GFP, red = marker of interest, blue = nuclei labeled with Toto-3. Co-expression of GFP and marker of interest is shown in yellow. (i-l) Confocal sections focused beneath the surface of the scaffold to examine mRPCs within the scaffold pores. (i) GFP fluorescence from mRPCs, (j) Cy3 fluorescence from anti-nf-200, (k) Toto-3 fluorescence from stained nuclei, and (l) overlay of panels i-k. (m-n) Cross-sections (20 μm thick) of an mRPC-PGS composite depicting (m) GFP fluorescence from mRPCs within pores and adhering to the surface of the polymer scaffold after 7 days in culture and (n) expression of nestin (overlay of fluorescence from GFP, Cy3 anti-nestin, and Toto-3). Bar = 40 μm.